Pflugers Arch - Eur J Physiol (2014) 466:1317–1327
DOI 10.1007/s00424-013-1365-2

Zebrafish and mouse TASK-2 K^+ channels are inhibited by increased CO_2 and intracellular acidification

Gaspar Peña-Münzenmayer · María Isabel Niemeyer · Francisco V. Sepúlveda · L. Pablo Cid

Received: 14 August 2013 / Revised: 12 September 2013 / Accepted: 13 September 2013 / Published online: 1 October 2013

Abstract TASK-2 is a K_{2P} K^+ channel considered as a candidate to mediate CO_2 sensing in central chemosensory neurons in mouse. Neuroepithelial cells in zebrafish gills sense CO_2 levels through an unidentified K_{2P} K^+ channel. We have now obtained zfTASK-2 from zebrafish gill tissue that is 49 % identical to mTASK-2. Like its mouse equivalent, it is gated both by extra- and intracellular pH being activated by alkalinization and inhibited by acidification. The pH_i dependence of zfTASK-2 is similar to that of mTASK-2, with $pK_{1/2}$ values of 7.9 and 8.0, respectively, but pH_o dependence occurs with a $pK_{1/2}$ of 8.8 (8.0 for mTASK-2) in line with the relatively alkaline plasma pH found in fish. Increasing CO_2 led to a rapid, concentration-dependent (IC_{50} ~1.5 % CO_2) inhibition of mouse and zfTASK-2 that could be resolved into an inhibition by intracellular acidification and a CO_2 effect independent of pH_i change. Indeed a CO_2 effect persisted despite using strongly buffered intracellular solutions abolishing any change in pH_i, was present in TASK-2-K245A mutant insensitive to pH_i, and also under carbonic anhydrase inhibition. The mechanism by which TASK-2 senses CO_2 is unknown but requires the presence of the 245–273 stretch of amino acids in the C terminus that comprises numerous basic amino acids and is important in TASK-2 G protein subunit binding and regulation of the channel. The described CO_2 effect might be of importance in the eventual roles played by TASK-2 in chemoreception in mouse and zebrafish.

Keywords K_{2P} K^+ channels · Zebrafish TASK-2 · Mouse TASK-2 · CO_2 · Intracellular pH

Introduction

Changes in arterial pCO_2 induce variations in pulmonary ventilation, with hypercapnia promoting an increase in ventilation. In mammals CO_2 levels are primarily sensed at central chemoreceptor neurons and although the primary function of the carotid body is to respond to changes in pO_2, it also contributes to CO_2 detection [16, 39]. Chemosensitive central neurons have been defined as those found in brainstem areas that are capable of responding to variations in CO_2/H^+ levels to signal ventilation changes [15]. Examples of those regions are the retrotrapezoid nucleus (RTN), the nucleus of the solitary tract, the locus coeruleus (LC) and caudal raphe nuclei [33]. Changes in CO_2/H^+ levels are transduced into changes in the firing response of chemoreceptor neurons [23, 39] and a great deal of work is being done to find the primary sensors involved. Depolarization, and therefore increase excitability of central pH-sensitive neurons has been shown to be linked to K^+ conductance inhibition and these channels are prime candidates to act as CO_2/H^+ sensors [31].

At least two types of K^+ channels have been proposed to be part of the cellular chemosensing apparatus. They are members of the background K_{2P} K^+ channel family [14] or they belong to the inwardly rectifying group of K^+ channels known as Kir [19]. Kir5.1 and Kir4.1 are prominently expressed in several brainstem nuclei involved in cardiorespiratory control [48] and coassembled, they are known to

Electronic supplementary material The online version of this article (doi:10.1007/s00424-013-1365-2) contains supplementary material, which is available to authorized users.

G. Peña-Münzenmayer · M. I. Niemeyer · F. V. Sepúlveda · L. P. Cid (✉)
Centro de Estudios Científicos (CECs), Avenida Arturo Prat 514, Valdivia, Chile
e-mail: pcid@cecs.cl

Present Address:
G. Peña-Münzenmayer
National Institute of Dental and Craniofacial Research, National Institutes of Health, 10 Center Drive, Bethesda, MD 20892, USA

form channels inhibited by hypercapnia, an effect mediated by intracellular acidification [49]. The possible role of Kir5.1/Kir4.1 channels in the respiratory response to hypercapnia has been explored through genetic inactivation of Kir5.1 in mice. Chemosensitive neurons of the LC from Kir5.1 KO animals become unresponsive to changes in cytoplasmic pH suggesting that Kir5.1 may be involved in the response to hypercapnic acidosis [13]; however, a study in the same animals shows that Kir5.1 channels are dispensable for functional central and peripheral respiratory chemosensitivity [44]. TASK subfamily K_{2P} channels TASK-1 and TASK-3, and TALK channel TASK-2 have been considered owing to their high sensitivity to extracellular pH. Simultaneous deletion of TASK-1 and TASK-3 in the mouse abolishes the acid-sensitive background K^+ current of raphe neurons, but the central ventilatory chemosensory response remains unaffected [32]. The involvement of TASK-1 or TASK-3 channels in the control of ventilation by peripheral chemoreceptors is a matter of controversy, with some authors implicating an important role for TASK-1 in carotid body response to hypoxia and hypercapnia [43], a notion not confirmed by more recent work [37].

TASK-2 [9], a TALK subfamily K_{2P} channel, is highly expressed in kidney proximal tubule cells where it plays a role in HCO_3^- reabsorption by virtue of its activation by extracellular alkalinization [47]. TASK-2 has a circumscribed brain expression notably in CO_2 chemosensitive RTN, and based on work with a TASK-2 KO mouse it has been proposed to be important in central CO_2 and O_2 chemosensitivity [17]. Interestingly, in addition to its extracellular pH sensitivity, TASK-2 has been shown to be regulated by intracellular pH thus offering a possible way to couple channel activity to CO_2 levels [35].

Fish are also able to respond to hypoxia and hypercapnia by regulating their ventilation rate that in this case corresponds to regulating water flow through the gill openings. The gill is also the main site of CO_2 sensing in fish and it has been hypothesized that gill chemoreceptors sensitive to external CO_2 rather than protons are capable of initiating a reflex mechanism leading to cardiovascular and respiratory adjustments (reviewed in [38]). Neuroepithelial cells (NECs) have been identified in the zebrafish gill and originally shown to respond to a decrease in O_2 level with inhibition of background-type K^+ channels and depolarization [24]. The same cells are sensitive to rather low levels of CO_2 [40], so that small increases in CO_2 inhibit background-type K^+ channels of similar characteristics as those sensitive to O_2, leading to CO_2-dependent NEC depolarization and presumably increased excitability. The response of NECs to CO_2 is only partially reduced (<50 %) by carbonic anhydrase inhibition [40]. Although this result suggests an effect of CO_2 secondary to its hydration and the predicted secondary acidification, the fact that a substantial CO_2 response persists could be interpreted to imply a direct effect. The same issue awaits a definite resolution in mammalian chemoreception, although it is known that the ventilatory response to hypercapnia is greater than that to metabolic acidosis and that central neurons exhibit a greater firing response to hypercapnic acidosis than isocapnic acidosis where the CO_2 levels remain constant and bicarbonate concentration and pH are decreased [46]. Also current clamp and intracellular pH recordings in neonatal rat brainstem slices show that the major signal in the chemosensitive response of LC neurons is pH_i rather than pH_o or CO_2 level [15].

If pH-sensitive K_{2P} channels are to take part in CO_2 chemoreception either in fish or mammals, it would appear that they will have to be inhibited by intracellular acidification or perhaps directly by increased CO_2 levels. The requirement for pH_i sensitivity discards TASK-1 and TASK-3 that are solely modulated by pH_o [14]. TASK-2, already proposed to have a function in central chemoreception in the mouse [17], on the other hand, would fulfill the pH_i-gating requirement [35]. In the present report we first identify a TASK-2 orthologue in zebrafish gill and provide a functional characterization. We then compare the response to CO_2 of TASK-2 channels from zebrafish and mouse origins, zfTASK-2 and mTASK-2. Both channels respond very similarly to CO_2, and the results suggest that part of the response is secondary to intracellular acidification but some pH_i-independent CO_2 sensitivity also forms part of the response. A difference in $pK_{1/2}$ for extracellular pH gating between zf and mTASK-2 might represent an adaptation to differing blood pH in fish and mammalian species.

Methods

Cloning and site directed mutagenesis

Danio rerio TASK-2 (zfTASK-2) was cloned from zebrafish gill by RT-PCR. Anesthesia by immersion in tricaine methanesulfonate (250 mg/ml) until cessation of opercular movements was followed by decapitation. Animal procedures were approved by the Institutional Animal Care and Use Committee of the Centro de Estudios Científicos. After dissection of the gill, total RNA was isolated with Trizol and 5 μg was reverse-transcribed using the SuperScript II system (Invitrogen) and oligo(dT) primer. Specific primers were designed to obtain the open reading frames (ORF) of two mTASK-2 orthologues accessible in the GenBank: zfTASK-2 (NP_001032478.1): 5′- AAGCTTACC**ATG**GTGGAC AAGGGACCTC-3′ and 5′-GGACAACACTGACATT**TAA** CTCGAG; and zfTASK-2b (NP_956927.1): 5′- AAGCTT GTATT**ATG**GCAGATAAAGGACC-3′ and 5′-GGAA AAGCTTTGGT**TGA**AGGACTCGAG- 3′. Data in bold are the start and stop codons. The *Hin*dIII and *Xho* I restriction sites (underlined) were incorporated to clone the ORFs in the mammalian expression vector pCR3.1. Mus musculus TASK-2 (K_{2P}5.1, GenBank accession no. AF319542) was that previously cloned from mouse kidney [34].The TASK-2 mutants

were generated by the quick-change method using KOD polymerase (Merck). mTASK-2-TASK-3 chimera (244TASK-2-245TASK-3) and the truncated mTASK-2Δ273 had been obtained before [35]. All the constructs were confirmed by sequencing.

Cell culture and transfections

HEK-293 cells were cultured in Dulbecco's modified Eagle's medium and F12 Ham's medium at 1:1 ratio, supplemented with 7 % fetal bovine serum at 37 °C in 5 % CO_2. For electrophysiological experiments, transient transfections of zfTASK-2, murine TASK-2 and mutants were done in HEK-293 cells as described previously using CD8 cotransfection to identify effectively transfected cells [8]. The CD8 antigen was revealed with microspheres (Dynabeads) coated with an anti-CD8 antigen.

Electrophysiology

When studying pH_o dependence, cells were seeded on 35-mm dishes and continuously superfused with a bathing solution containing 67.5 mM Na_2SO_4, 4 mM KCl, 1 mM K-gluconate, 2 mM $CaCl_2$, 1 mM $MgCl_2$, 10 mM HEPES/Tris pH 7.5. Osmolality was adjusted with sucrose to a final value of 310 mOsm. Pipette solution contained 132 mM K-gluconate, 8 mM KCl, 1 mM $MgCl_2$, 10 mM EGTA, 1 mM Na_3ATP, 0.1 mM GTP, 10 mM HEPES/Tris pH 7.5, 300 mOsm. Standard whole-cell patch clamp recordings were done as described elsewhere [34]. Experiments were performed at room temperature using a holding potential of −70 mV. Currents were measured at several potentials, but data reported are generally those obtained at 0 mV.

In experiments designed to measure the extracellular pH dependence of the currents, bathing solutions contained HEPES (4-(2-hydroxyethyl) piperazine-1-ethanesulfonic acid) for pH 7.0, 7.5 and 8.0; AMPSO (*N*-(1,1-dimethyl-2-hydroxyethyl)-3-amino-hydroxypropanesulfonic acid) for pH 8.5 and 9.0; CAPS (3-(cyclohexylamino)-1-propanesulfonic acid) for pH 9.5, 10, 10.5 and 11; or MES (2-(*N*-morpholino)-ethanesulfonic acid) for pH 6.0 and 6.5. The intracellular pH dependence of the currents was measured using the pH_i clamp method modifying the transmembrane concentration gradient for acetate as described previously [50]. The composition of the solutions is exactly as previously described [35]. A pulse of 10 mM NH_4Cl was used to produce intracellular alkalinization.

To measure CO_2 dependence a low buffering power pipette solution contained 132 mM K-gluconate, 8 mM KCl, 1 mM $MgCl_2$, 10 mM EGTA, 1 mM HEPES/Tris, 1 mM Na_3ATP, 0.1 mM GTP, pH 7.5. For a highly buffered pipette solution, 100 mM KCl was replaced by 100 mM HEPES-K and pH 7.5 was reached with H_2SO_4. Additionally, 20 μM EZA (6-ethoxyzolamide, Sigma) was used in some experiments to inhibit intracellular carbonic anhydrases. These solutions were adjusted to pH 7.5. Control bathing solution contained 135 mM Nagluconate, 4 mM KCl, 1 mM K-gluconate, 2 mM $CaCl_2$, 1 mM $MgCl_2$, 30 mM HEPES/Tris pH 7.5. CO_2 containing bath solutions were made by replacing 6, 33 or 150 mM Nagluconate with $NaHCO_3$. To obtain a pH of 7.5 they were bubbled with 1 %, 5 % or 25 % CO_2/O_2 mixtures, respectively. To measure a possible modulation of the currents by O_2, an HCO_3^--free bathing solution bubbled with 100 % O_2 was used.

Intracellular pH measurements

HEK-293 cells were mounted in an inverted microscope (IX70 Olympus) equipped with a 40× oil immersion objective, a Xenon lamp, an Optoscan Monochromator and a photomultiplier system (Cairn Research). Cells were dialyzed with a pipette solution containing 100 μM of 2′,7′-bis-(2-carboxyethyl)-5-(and −6)-carboxyfluorescein (BCECF) free acid in the whole cell configuration. Excitation wavelengths were alternated between 440 and 490 nm and emission was collected at 535 nm. The demultiplexed signal was acquired with an analog–digital interface (Digidata 1200; Axon Instruments) and monitored using the pCLAMP 10 software (Axon Instruments). Intracellular pH calibration curves (Fig. S1a) were obtained at the end of experiments by the high potassium nigericin calibration method as described previously [50]. When this was not possible, intracellular pH was calculated using a one-point calibration method [4, 6] as follows: cells were exposed to a pH 7.0 calibration solution containing 140 mM K-gluconate and 10 μM nigericin. The ratio 490/440 from the entire experiment was divided by the pH 7.0 490/440 ratio and intracellular pH was calculated using the parameters from the calibration curves.

Simultaneous measurements of currents and pH_i

Standard whole cell patch clamp experiments were performed using a pipette solution containing 100 μM BCECF free acid. HEK-293 cells expressing mTASK-2 or zfTASK-2 were exposed to bathing solutions containing 1 %, 5 % or 25 % CO_2. K^+ currents were monitored simultaneously with intracellular pH. Pipette bathing solutions contained 1 or 100 mM HEPES to obtain a low or a high intracellular buffering power, respectively. Alternatively, 20 μM EZA was used in the pipette solution in order to block intracellular carbonic anhydrases.

Results

Zebrafish TASK-2 orthologues from gill tissue

A database search for zebrafish orthologues of mTASK-2 revealed two target sequences which are probably paralogues.

We obtained both cDNAs by RT-PCR amplification of gill total RNA using specific primers. The predicted polypeptide sequences were 513 (zfTASK-2) and 448 (zfTASK-2b) amino acids long. Figure 1 shows an alignment of both zebrafish sequences along with mTASK-2. The overall identity between zebrafish paralogues is 46 %, but it increases to 68.3 % if amino acids 1–240 that encompass the four transmembrane domains (TM) and the two pore segments (P) are considered. Comparison of mTASK-2 (502 amino acids) with zfTASK-2 gave an overall identity of 49.4 % increasing to 73.3 % for amino acids 1–240. The same comparison done with zfTASK-2b gave respective identities of 40.7 % and 64.6 %. In the distal intracellular segment, from amino acid 241 to the end of the sequence, identity decreases to 28.6 % and 18.6 % when comparing mTASK-2 with zfTASK-2 and zfTASK-2b, respectively. Mammalian TASK-2 is gated both by extra- and intracellular pH and arginine 224 and lysine 245 have been identified as respective sensors in these processes [35, 36]. Both sensor amino acids are conserved in zfTASK-2, but in zfTASK-2b the lysine 245 is changed to asparagine.

Attempts to express zfTASK-2b in HEK-293 cells failed to induce any currents and the mechanism for this lack of function has not been explored further. Expression of zfTASK-2, on the other hand, was accompanied by the appearance of voltage-independent instantaneous K^+ currents accompanied by a further voltage-dependent component (Fig. 2a and b) typical of K_{2P} TASK-2 channels described before. The steady-state IV relations approached open rectification (Fig. 2c). Figure 2d shows the response of zfTASK-2 currents recorded at 0 mV to graded changes in extracellular pH. A large activation was seen upon switching from pH 7.5 to 11.0, which was reversed gradually as the pH was again decreased with current inhibition at pH 6.0. This activation by alkalinization, typical of TALK K_{2P} family members, occurred with a $pK_{1/2}$ of 8.82±0.07 and a Hill coefficient of 0.81±0.08 (means±SEM, $n=5$). This last figure did not differ from unity (t-test, $P=0.0764$). A series of concurrently done measurements with mouse TASK-2 gave $pK_{1/2}$ of 8.03±0.11 (mean±SEM, $n=6$) that does not differ from previously published figures [34, 41]. Despite conservation of mouse pH_o-sensing R224 the sensitivity of zfTASK-2 to pH_o is alkaline-displaced almost a full pH unit. As argued before, change in the environment of the sensor might strongly influence its pK_a and we have mutated some non-conserved amino acids of zfTASK-2 that might affect R224 to the residues present in mTASK-2 [36]. The following mutations of zfTASK-2 were without effect on the pH_o dependence: D77N, V78M, K78Q and P220N. Double mutation D214N-E218N and single I104V change shifted zfTASK-2 $pK_{1/2}$ to 8.59±0.06 ($n=4$) and 8.36±0.03 ($n=3$), respectively.

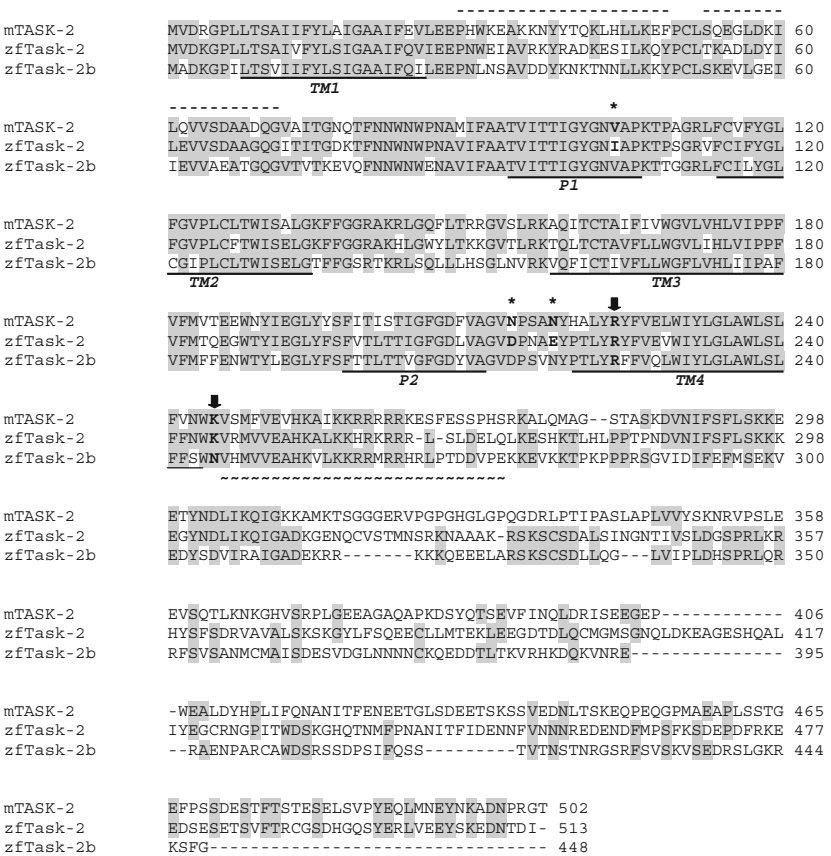

Fig. 1 Alignment of deduced amino acid sequences of zfTASK-2 paralogues and mTASK-2. Identical amino acids are shown in *gray*. Amino acids forming the extracellular helical cap helices are identified by the *upper discontinuous line* (—). The extracellular and intracellular pH sensors R224 and K245 are indicated by *arrows*. Notice the K245N change in zfTASK-2b. Also highlighted (*) are zfTASK-2 non-conserved amino acids that when mutated to the mouse equivalents partially reversed the alkaline shift observed for the $pK_{1/2}$ for pH_o-gating of zfTASK-2, and a region (~) that appears essential for the CO_2 effect

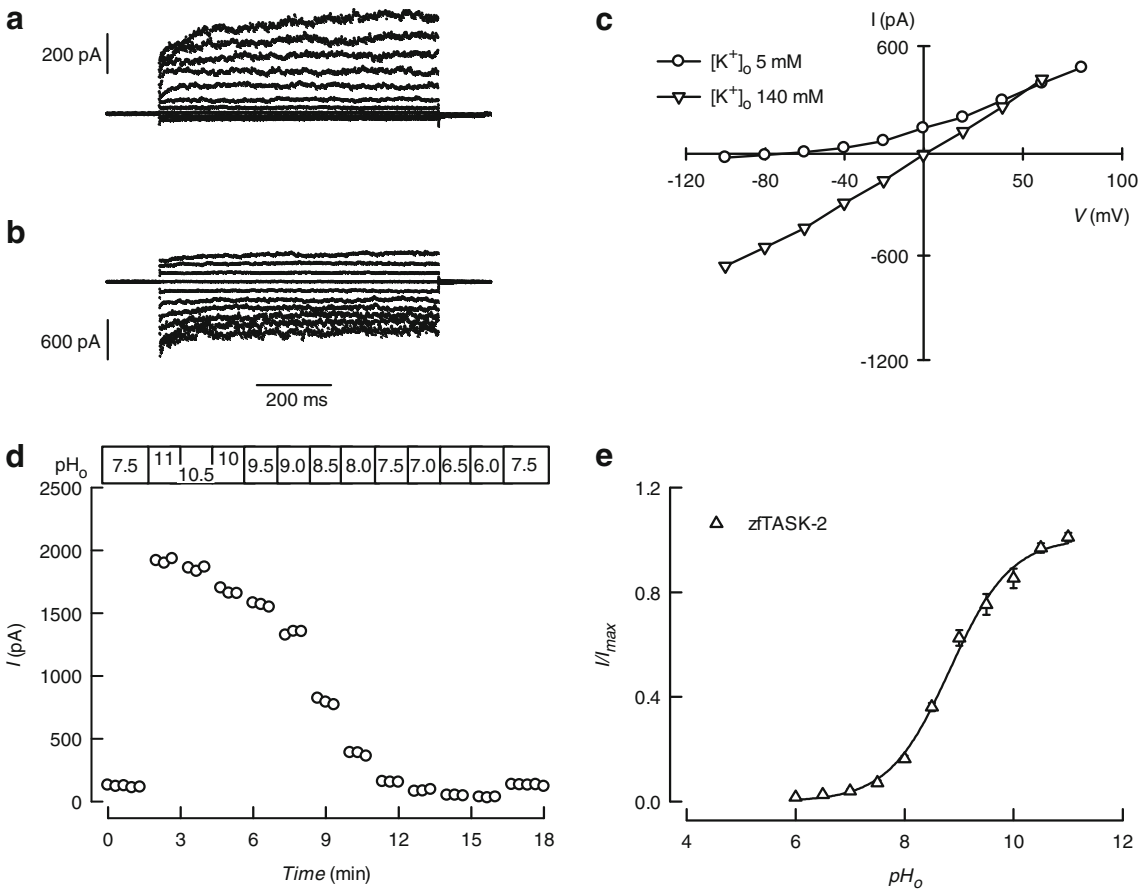

Fig. 2 zfTASK-2 potassium channels are activated by extracellular alkalinization. Currents were recorded in HEK-293 cells after transfection with zfTASK-2 cDNA by the whole-cell mode of the patch-clamp technique. **a**, **b** Current traces obtained at 5 and 140 mM extracellular [K^+], respectively, in a cell containing 140 mM intracellular [K^+]. Square voltage pulses delivered from holding voltages of −70 mV (**a**) and 0 mV (**b**) ranged from −100 to 80 mV in 20-mV steps. **c** Current–voltage relationships corresponding to experiments in **a** and **b** based on measurements at the end of the pulses. **d** Time course of zfTASK-2-mediated current recorded at 0 mV with $[K^+]_i/[K^+]_o$ 140/5 mM in response to changes in extracellular pH values. **e** Average extracellular pH dependence curve of zfTASK-2 (mean±SEM, $n=5$). The line is a fit of the Hill equation and was constructed by using the average of fitted parameters of the individual experiments. Parameters were 8.82±0.07 and 0.81±0.08 for $pK_{1/2}$ and n_H, respectively (means±SEM, $n=5$). Respective values previously measured for mTASK-2 were 8.03±0.11 and 0.85±0.06 [36]

We have previously shown that mTASK-2 is also pH_i-gated with a $pK_{1/2}$ of 8.0 [35]. Using intracellular acetate and BAPTA to buffer Ca^{2+}, it is possible to change pH_i predictably by changing extracellular acetate. Figure 3a shows the effect of clamping pH_i at values between 7.0 and 9.0 on K^+ current of a zfTASK-2-expressing HEK-293 cell. This was achieved by changing $[acetate^-]_o$ between 1.26 and 126 mM with $[acetate^-]_i$ of 50 mM. Current mediated by zfTASK-2 was greatly increased by alkalinization from to pH_i 7.4 to 9.0 with a graded decrease in the current as pH_i was lowered to 7.0, the lowest pH attainable with this set of acetate concentrations. Using $[acetate^-]_i$ values of 10 and 130 mM, it is possible to extend the range of pH_i values achieved down to 6.3 and up to 9.5, respectively. This approach allowed composing Fig. 3b out of 27 experiments. Fit of a Hill equation to the data yielded a $pK_{1/2}$ value of 7.9±0.05 and n_H of 0.8±0.09 (parameters±SEM, obtained from the fit); this last value is not different from unity (t-test, $P=0.147$). These values were not different from those of the mouse orthologue, $pK_{1/2}$ of 8.0±0.07 and n_H of 0.9±0.04 [35].

CO_2 sensitivity of mouse and zebrafish TASK-2

TASK-2 channels have been proposed to be important in mediating central O_2/CO_2 chemosensitivity in mice [17] while a background K^+ channel, conceivably zfTASK-2 cloned here, is involved in CO_2 sensing in NEC cells of zebrafish gills [40]. CO_2 exerts an effect on mTASK-2 that has been attributed to an intracellular acidification secondary to its permeation into the cell and subsequent carbonic anhydrase-catalyzed hydration [35]. A direct effect of CO_2 on the channel cannot, however, be discarded. We have examined the effect of increasing levels of CO_2 on mouse and zfTASK-2 (Fig. 4a and b), both of which responded with graded inhibition that was reversed as the solution was returned to nominally CO_2-

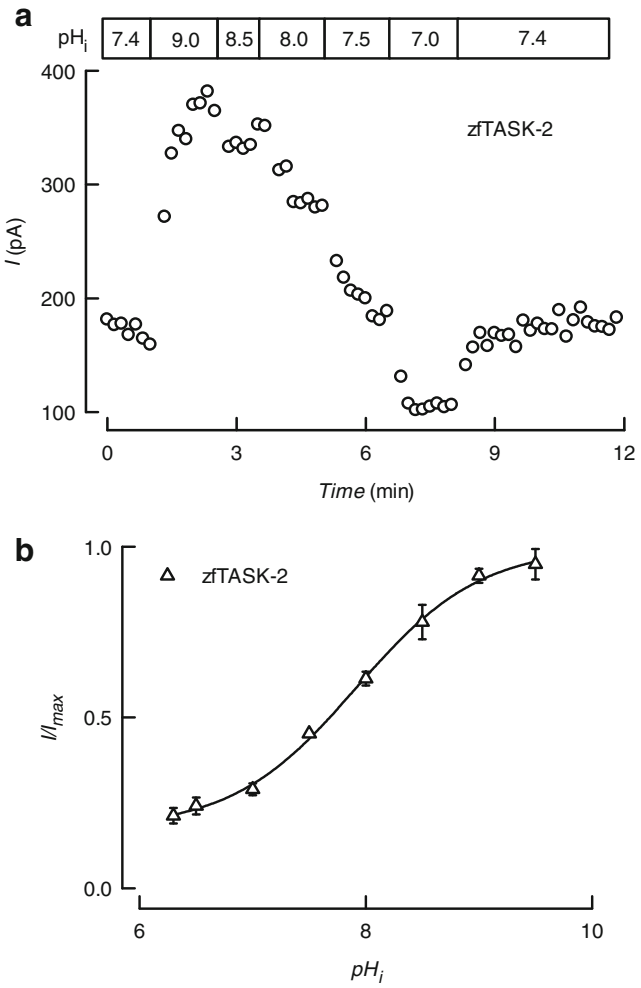

Fig. 3 Effect of intracellular pH on zfTASK-2-mediated currents. **a** Time course of zfTASK-2-mediated current recorded at 0 mV at various indicated pH_i values. The cell had 50 mM intracellular acetate and extracellular acetate concentrations were changed from 1.26 to 126 mM to yield pH_i values ranging from7.0 to 9.0 [35]. Extracellular pH was 7.4 throughout. **b** summary of experiments examining the pH_i dependence of zfTASK-2 (means±SEM, n=9–27). The full range of pH values shown were attained using intracellular solutions with 10 or 130 mM acetate to reach pH_i values down to 6.3 and up to 9.5, respectively. To analyze together the three sets of data, each group was normalized to the value of current attained with pH_i 7.0. The line shows a fit of a Hill function to the data that gave a $pK_{1/2}$ of 7.9±0.05 and n_H 0.8±0.09 (parameters±SEM, obtained from the fit)

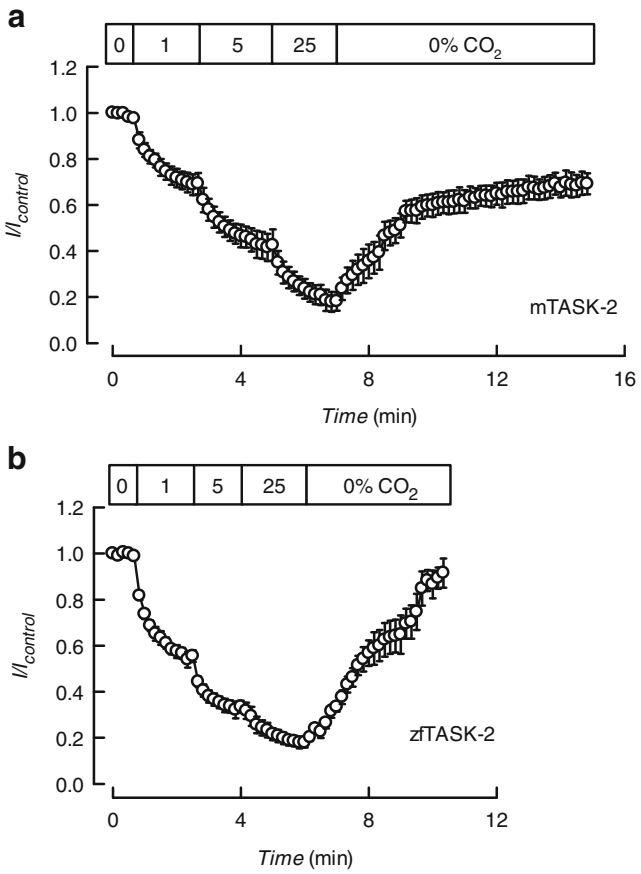

Fig. 4 TASK-2 channels are inhibited by CO_2 in a dose-dependent manner. Time course of currents recorded at 0 mV at the indicated CO_2 concentrations in **a** mTASK-2-expressing HEK-293 cells (n=6) and in **b** zfTASK-2-expressing HEK-293 cells (n=5). The extracellular pH was maintained at 7.5 in 1 %, 5 % and 25 % CO_2 saturated solutions with bicarbonate concentrations of 6, 33 and 150 mM HCO_3^-, respectively. The results are means±SEM In all experiments the intracellular solution was weakly buffered with 1 mM HEPES

free solution. These experiments were carried out using CO_2/O_2 gas mixtures, but O_2 by itself was found to have no effect on TASK-2 (Fig. S2a). Changes in cell volume regulate the activity of TASK-2 [34], but no such changes occur during CO_2 challenge of TASK-2-expressing cells (Fig. S2b).

Separate experiments using intracellular BCECF show that exposure of HEK-293 cells to 1 %, 5 % and 25 % CO_2 decreased pH_i from 7.37±0.12 to 6.95±0.05, 6.43±0.05 and 6.10±0.06, respectively (means±SEM; see also Fig. S1c). The initial pH_i found experimentally lies below the $pK_{1/2}$ value for intracellular gating of the TASK-2 channels, nevertheless around 25 % of the maximal activity is predicted, leaving room for further inhibition by acidification. It could therefore be surmised that the CO_2 inhibition observed in mouse and zfTASK-2 is the exclusive consequence of intracellular acidification.

To approach the question of whether CO_2 effect is due solely to changes in pH_i we have used strongly buffered intracellular solutions. Figure 5a compares the effect of extracellular superfusing the weak base NH_4Cl on cells that contain 1 mM intracellular HEPES or strongly buffered cells containing 100 mM HEPES. Influx of the highly permeable NH_3 ought to lead to an increase in pH_i when intracellular NH_4^+ is formed again by NH_3 capture of protons [42]. An immediate increase in K^+ current following a NH_4Cl pulse was observed in cells containing 1 mM intracellular HEPES, but the response was greatly diminished in cells containing 100 mM buffer. This suggests that the NH_4Cl pulse was able to alkalinize cells and that strong buffering with 100 mM intracellular HEPES largely attenuated the change in pH_i. Figure 5b shows a similar experiment but using CO_2 to acidify intracellularly. Although the

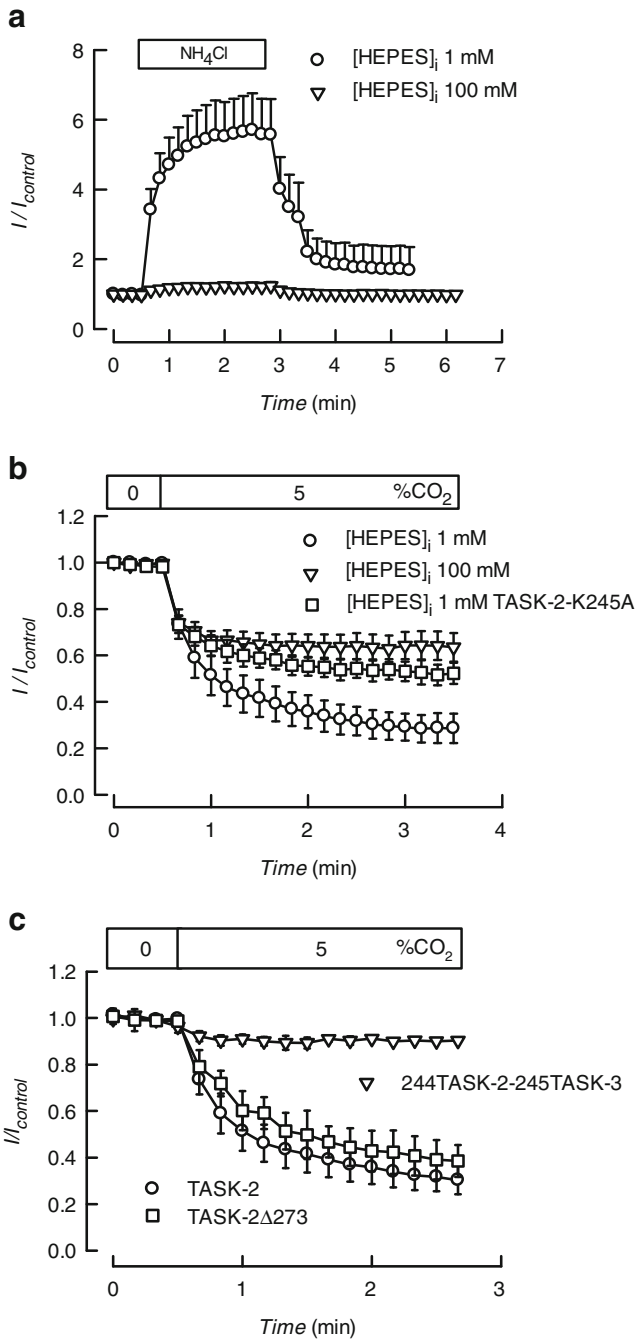

◀ **Fig. 5** Effect of increased buffering capacity on TASK-2 response to ammonium and CO_2 pulses. **a** Time course of currents recorded at 0 mV in mTASK-2-expressing HEK-293 cells. During the time indicated, the solution bathing the cells was switched to one containing 10 mM NH_4Cl to elicit intracellular alkalinization. The activation of the channel activity observed when the pipette solution was buffered with 1 mM HEPES (*circles*, $n=8$) was strongly inhibited by increasing HEPES concentration in the pipette solution 100 mM (*triangles*, $n=7$). **b** An analogous experiment but using a bath solution saturated with 5 % CO_2 and containing 33 mM HCO_3^-. The inhibition observed when the pipette solution contained 1 mM HEPES (*circles*, $n=8$) was partially impeded when the intracellular buffer capacity was increased using 100 mM HEPES (*triangles*, $n=8$). Squares show the results obtained with 1 mM intracellular HEPES in cells expressing the mTASK-2-K245A pH_i-insensitive mutant ($n=5$). Extracellular pH was 7.5 throughout and the results are means±SEM. **c** Comparison of the effect of 5 % CO_2 on currents mediated by mTASK-2 (*circles*, $n=8$), a mutant truncated in its C terminus end mTASK-2-Δ273 (*squares*, $n=3$) and 244TASK-2-245TASK-3 chimera, that has the C terminus of pH_i-insensitive TASK-3 (*triangles*, $n=3$)

response to the predicted decrease in pH_i is reduced when strongly buffered pipette solution was used, we observed a sizable effect that could be attributed to a direct effect of CO_2 if no change in pH_i were taking place. Neutralization of lysine 245 of mTASK-2 abolishes pH_i sensitivity [35]. A chimera where C terminus amino acids starting at residue 244 of TASK-2 are replaced by the C-terminal residues 245–365 of the pH_i-insensitive TASK-3 channel [244TASK-2-245TASK-3, 35] was unresponsive to CO_2. A construct we have termed TASK-2Δ273, which lacks C-terminal amino acids from residue 273 down and shows unaltered response to changes in pH_i [35], responded to CO_2 as the non-mutated TASK-2 (Fig. 5c). The stretch from aa 245 to 273 therefore appears essential for CO_2 sensing in TASK-2. Silencing of the pH_i sensor itself as in mutant TASK-2-K245A only decreased the effect of CO_2 to the level observed with strong pH_i buffering (Fig. 5b).

To explore further the possibility of an effect of CO_2 that is separate from its predicted intracellular acidification response, we measured TASK-2-mediated current and pH_i simultaneously in weakly or strongly buffered cells, we additionally inhibited carbonic anhydrase and utilized a TASK-2 mutant with pH_i and pH_o sensors disabled by mutation.

Measurements of K^+ currents and pH_i are summarized in Fig. 6a and b. In Fig. 6a, a graded increase in CO_2 is shown to produce a marked inhibition in current in a weakly buffered cell expressing mTASK-2 which coincides with a marked intracellular acidification (Fig. 6b). To attempt to impede the drop in pH_i, cells were strongly buffered with 100 mM HEPES and were additionally dialyzed with 20 μM ethoxyzolamide (EZA) to inhibit carbonic anhydrase. Under these conditions the CO_2-induced acidification was abolished, yet a sizable inhibition of current still took place (Fig. 6a and b). In Fig. 6c, these data are replotted, together with an experiment carried out in zfTASK-2-expressing cells, to emphasize the fact that under strong pH_i buffering and additional carbonic anhydrase inhibition there was an up to 50 % inhibition of K^+ current by CO_2 without any measurable change in pH_i.

To ascertain whether the pH_i-independent effect exerted by CO_2 on TASK-2 activity requires the pH-sensing machinery of the channel, we used a mutant, mTASK-2-R224A-K245A, in which both extracellular and intracellular pH sensors are disabled. In Fig. 7, the effect of increasing CO_2 from nominally zero to 1 %, 5 % and 25 % is seen to produce an effect on mTASK-2-R224A-K245A-mediated current that can be superposed on that elicited by CO_2 under strongly buffered intracellular pH in wild-type mTASK-2-expressing cells.

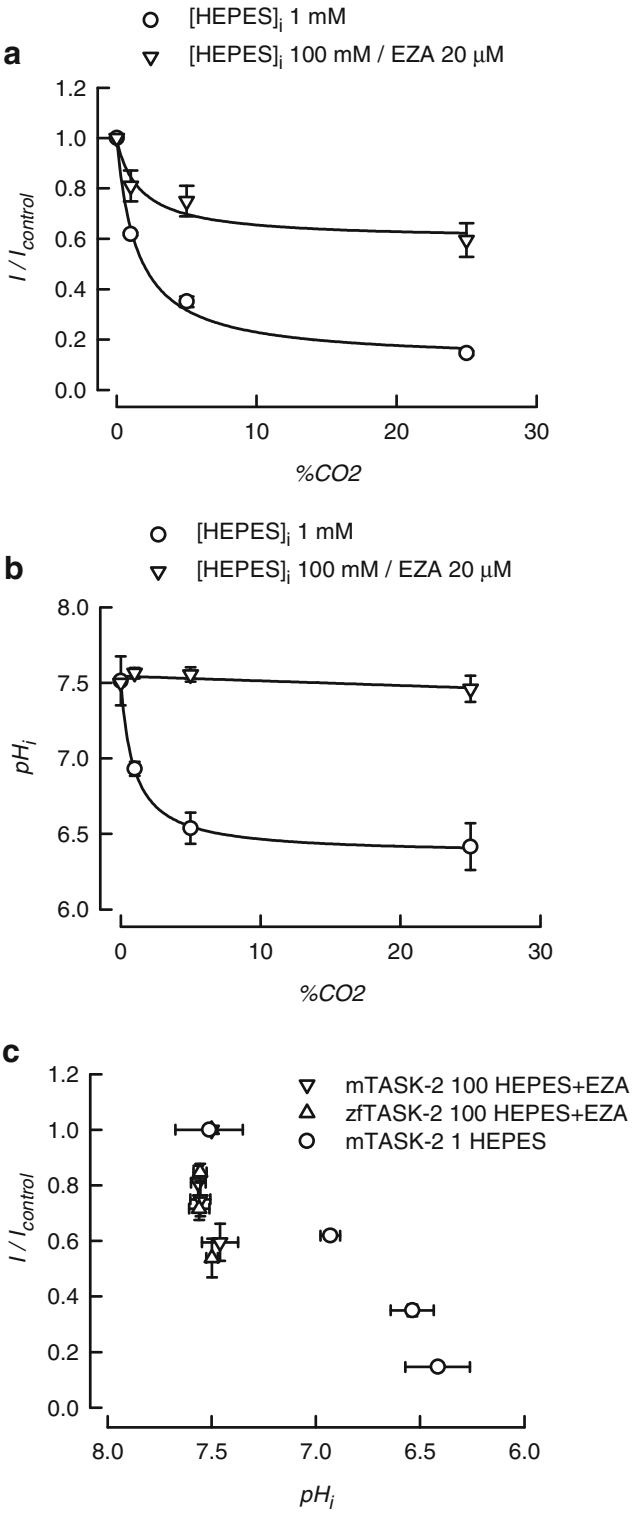

◀ **Fig. 6** Simultaneous measurement of ion current and intracellular pH reveals pH_i-independent inhibition of mTASK-2 by CO_2. **a** mTASK-2 current inhibition by increasing CO_2 measured with low intracellular buffer capacity (*circles*, $n=5$) or with strong buffering with 100 mM HEPES and additional inhibition of carbonic anhydrase with 20 μM intracellular EZA (*triangles*, $n=3$). **b** Simultaneously measured intracellular pH using fluorescent pH indicator BCECF. **c** Replottting the data in **a** and **b** as current versus pH_i to show that using 100 mM HEPES and 20 μM a EZA sizable change in current occurred without concomitant change in pH_i. Data for zfTASK-2 obtained using an intracellular solution containing 100 mM HEPES and 20 μM EZA are also shown ($n=7$). Results are means±SEM

Discussion

We have identified a zebrafish (*D. rerio*) orthologue of K_{2P} TASK-2 K^+ channel isolated from gill tissue. zfTASK-2 is 49 % identical to its mouse equivalent and, like mTASK-2, is gated both by extra- and intracellular pH. NECs in zebrafish, and presumably other fish, are capable of sensing O_2 and CO_2 levels, and do so through the modulation of a conductance exhibiting the characteristics of K_{2P} background K^+ channels [1, 24, 30]. TASK-1, TASK-3 and TASK-2 are K_{2P} channels that have been considered as candidates to play roles in CO_2 sensing in central and peripheral chemosensory neurons in mammals [17, 32, 37, 43]. Of these, only TASK-2 is sensitive to intracellular pH, being inhibited by acidification and further activated by alkalinization with a $pK_{1/2}$ of 8.0 [35], making it a plausible candidate to sense CO_2 levels through its hydration and consequent intracellular acidification. Mammalian K_{2P} channels sharing the property of being regulated by intracellular pH, and also present in zebrafish [18], are TREK-1 and TREK-2, but they are activated by acidification [27, 29], and TRAAK that is not inhibited by acidification [25]. TWIK-1and −2 are inhibited by 100 % CO_2 but there is no evidence for a direct effect of pH_i [7, 26]. This leaves TASK-2, and eventually its relatives TALK-1 and −2, as sole K_{2P} candidates able to sense a CO_2-dependent acidification with inhibition leading to depolarization and increased excitability.

Functional expression of zfTASK-2 yields currents with similar time- and voltage-independence as those observed for

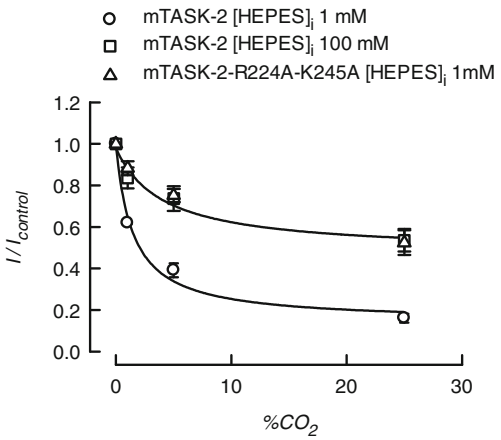

Fig. 7 Effect of CO_2 on pH_o- and pH_i-insensitive mTASK-2-R224A-K245A mutant. Data (*triangles*) for the mutant mTASK-2 were collected using 1 mM intracellular HEPES and are means±SEM ($n=6$). Data for wild-type mTASK-2 with 1 or 100 mM intracellular HEPES are also shown for comparison

its mouse orthologue. A voltage-dependent component of otherwise instantaneous currents might be attributed to voltage-related changes in occupancy of the selectivity filter affecting pore opening. Indeed, the $pK_{1/2}$ of extracellular pH-gating has been seen to be dependent on K^+ concentration and voltage in mTASK-2 [9]. Zebrafish TASK-2, like mTASK-2, is inhibited by intra- and extracellular acidification and activated by intra- and extracellular alkalinization. zfTASK-2 pH_i dependence, with a $pK_{1/2}$ of 7.9, is quite similar to that of mTASK-2 [35]. There are no data on intracellular pH in adult zebrafish, but measurements with a fluorescent indicator in early embryos give a figure of 7.55 [30]. This is 0.3–0.4 pH units more alkaline than pH measurements in muscle tissue of adult fish of various species (cited in [30]). It must be said that these last measurements lacked cellular resolution.

In contrast to the similarity in pH_i-gating between zebrafish and mouse TASK-2, the dependence of zfTASK-2-currents on pH_o occurred with a $pK_{1/2}$ of 8.82, which compares with a value of 8.0 observed for mTASK-2 [36]. This large alkaline displacement in pH_o dependence in zfTASK-2 correlates well with the relatively alkaline plasma pH observed in fish compared with that of mammals. Again, in zebrafish embryos, an "interstitial" pH value of 8.08 has been reported [30], while examples of measurements of adult fish aortic plasma pH give values of 7.91 in carp [10] and 8.08 in rainbow trout [21]. We have explored the possible reason for the alkaline displacement in zfTASK-2 pH_o dependence and have some inkling that differences in amino acids near the pH_o sensor might be responsible. Regardless of the mechanism involved, the change in $pK_{1/2}$ could be an adaptation to the markedly more alkaline extracellular pH in fish compared to mammals.

The question of whether a putative CO_2 K^+ channel sensor fulfills its signaling function through a change in activity in direct response to a change in CO_2 levels, or does so secondarily through intracellular acidification, remains open. Given the possibility that mTASK-2 and zfTASK-2 play such a role in mammalian chemoreceptor neurons and gill NECs, respectively, we have tried to discern if CO_2 sensitivity is direct or a function of changes in pH_i.

Increasing CO_2 led to a rapid, concentration-dependent inhibition of mouse and zfTASK-2. Perhaps surprisingly the response of zfTASK-2 to graded increases in CO_2 level was not much different from that of mTASK-2, considering that air breathers have arterial blood levels of CO_2 that are around one order of magnitude higher than fish [38]. This would appear to contradict a role of zfTASK-2 in NEC CO_2 sensing, but the participation of a different component complementing the channel to form a molecular sensing unit cannot be discarded. In fact, carbonic anhydrases have often been proposed to interact functionally with membrane transport proteins in so called metabolons, as first proposed for the association of anion exchanger and carbonic anhydrase in red cells [45] and recently in zebrafish gill cells involved in Na^+ transport [22].[1] Establishing whether such interaction between carbonic anhydrase and zfTASK-2 might be important in CO_2 sensing will require experimentation with native NECs.

The effect of CO_2 on mTASK-2 and zfTASK-2 appear indistinguishable. Additional dissection of the effect allows resolving two components to CO_2 inhibition: one related to channel inhibition by intracellular acidification and a second that takes place in the absence of acidification and must pertain to a more direct type of CO_2 effect. This view is based on three observations. (1) Use of strongly buffered intracellular solutions that abolish any change in pH_i does not preclude CO_2-dependent inhibition of TASK-2-mediated currents. (2) Neutralization of lysine 245 of mTASK-2, that abolishes pH_i-sensitivity of the channel [35], did not abolish the effect of CO_2 but just decreased to the level observed with strong pH_i-buffering. (3) Use of a carbonic anhydrase inhibitor did not abolish the CO_2 effect on TASK-2 activity but reduced it to the levels observed when changes in pH_i were impeded by using highly buffered intracellular solutions.

The mechanism by which TASK-2 of either murine or zebrafish origin sense CO_2 will have to be the subject of future investigation. The effect of CO_2 might be a direct action on the channel. The other possibility is the participation of a different sensing partner that couples functionally to the channel as has been proposed for K^+ channels involved in O_2 sensing [28]. A direct effect of CO_2 has been proposed to regulate an unidentified K^+ inwardly rectifying channel of Hela cells, but this is activated by CO_2 [20]. Enzymes using CO_2 as substrate must have binding sites allowing CO_2–protein interaction. An example of these is phosphoenolpyruvate carboxykinase that catalyzes the carboxylation of phosphoenolpyruvate to oxaloacetate and whose crystal structure has revealed CO_2 hydrogen bonding with basic amino acid side chains [11]. Indeed, examination of a range of proteins has established a so-called CO_2 formatics that suggests how proteins bind CO_2 and in which basic amino acids feature prominently [12]. The apparently direct effect of CO_2 on TASK-2 described here requires the presence of a stretch of amino acids in the C terminus going from residue 245 to 273. Whether this portion of the protein is necessary to CO_2 sensing by TASK-2 or for interaction with a sensing partner is not known at present. Interestingly this stretch of C terminus sequence is rich in basic amino acids that have been proposed to be important determinants of TASK-2 G protein subunit binding and regulation of the channel [3]. That CO_2 might interact with that process easily comes to mind, particularly since in preliminary experiments we have been unable to see an effect of CO_2 added to the intracellular aspect of inside-out membrane patches (Fig. S2c). Independently of the mechanism involved, however, our data indicate that CO_2 can inhibit TASK-2 background K^+ channels by a possibly

[1] Notice that there are dissenting views on the validity of the metabolon concept [2, 5].

direct effect not connected to intracellular acidification. This observation, in addition to representing a novel type of regulation for K^+ channels, might be of importance for the eventual roles played by TASK-2 in chemoreception in mouse and zebrafish.

Acknowledgments This work was supported by FONDECYT grant 1110774. The Centro de Estudios Científicos (CECs) is funded by Centers of Excellence Base Financing Program of Conicyt. We are grateful to Dr. Wendy González (Talca) for her help with molecular modeling work and to Carlos Bórquez for his assistance.

References

1. Abdallah SJ, Perry SF, Jonz MG (2012) CO_2 signaling in chemosensory neuroepithelial cells of the zebrafish gill filaments: role of intracellular Ca^{2+} and pH. Adv Exp Med Biol 758:143–148
2. Al-Samir S, Papadopoulos S, Scheibe RJ, Meissner JD, Cartron JP, Sly WS, Alper SL, Gros G, Endeward V (2013) Activity and distribution of intracellular carbonic anhydrase II and their effects on the transport activity of anion exchanger AE1/SLC4A1. J Physiol. doi: 10.1113/jphysiol.2013.251181
3. Añazco C, Peña-Münzenmayer G, Araya C, Cid LP, Sepúlveda FV, Niemeyer MI (2013) G protein modulation of K_{2P} potassium channel TASK-2: a role of basic residues in the C-terminus domain. Pflugers Arch. doi:10.1007/s00424-013-1314-0
4. Baxter KA, Church J (1996) Characterization of acid extrusion mechanisms in cultured fetal rat hippocampal neurones. J Physiol 493:457–470
5. Boron WF (2010) Evaluating the role of carbonic anhydrases in the transport of HCO_3^--related species. Biochim Biophys Acta 1804:410–421
6. Boyarsky G, Ganz MB, Sterzel RB, Boron WF (1988) pH regulation in single glomerular mesangial cells: I. Acid extrusion in absence and presence of HCO_3^-. Am J Physiol 255:C844–C856
7. Chávez RA, Gray AT, Zhao BB, Kindler CH, Mazurek MJ, Mehta Y, Forsayeth JR, Yost CS (1999) TWIK-2, a new weak inward rectifying member of the tandem pore domain potassium channel family. J Biol Chem 274:7887–7892
8. Cid LP, Niemeyer MI, Ramírez A, Sepúlveda FV (2000) Splice variants of a ClC-2 chloride channel with differing functional characteristics. Am J Physiol 279:C1198–C1210
9. Cid LP, Roa-Rojas HA, Niemeyer MI, González W, Araki M, Araki K, Sepúlveda FV (2013) TASK-2: a K_{2P} K^+ channel with complex regulation and diverse physiological functions. Frontiers in Physiology 4:doi: 10.3389/fphys.2013.00198
10. Claiborne JB, Heisler N (1986) Acid–base regulation and ion transfers in the carp (*Cyprinus carpio*): pH compensation during graded long- and short-term environmental hypercapnia, and the effect of bicarbonate infusion. J Exp Biol 126:41–61
11. Cotelesage JJ, Puttick J, Goldie H, Rajabi B, Novakovski B, Delbaere LT (2007) How does an enzyme recognize CO_2? Int J Biochem Cell Biol 39:1204–1210
12. Cundari TR, Wilson AK, Drummond ML, Gonzalez HE, Jorgensen KR, Payne S, Braunfeld J, De JM, Johnson VM (2009) CO_2-formatics: how do proteins bind carbon dioxide? J Chem Inf Model 49:2111–2115
13. D'Adamo MC, Shang L, Imbrici P, Brown SD, Pessia M, Tucker SJ (2011) Genetic inactivation of Kcnj16 identifies Kir5.1 as an important determinant of neuronal PCO_2/pH sensitivity. J Biol Chem 286: 192–198
14. Enyedi P, Czirják G (2010) Molecular background of leak K^+ currents: two-pore domain potassium channels. Physiol Rev 90:559–605
15. Filosa JA, Dean JB, Putnam RW (2002) Role of intracellular and extracellular pH in the chemosensitive response of rat locus coeruleus neurones. J Physiol 541:493–509
16. Forster HV, Martino P, Hodges M, Krause K, Bonis J, Davis S, Pan L (2008) The carotid chemoreceptors are a major determinant of ventilatory CO_2 sensitivity and of P_aCO_2 during eupneic breathing. Adv Exp Med Biol 605:322–326
17. Gestreau C, Heitzmann D, Thomas J, Dubreuil V, Bandulik S, Reichold M, Bendahhou S, Pierson P, Sterner C, Peyronnet-Roux J, Benfriha C, Tegtmeier I, Ehnes H, Georgieff M, Lesage F, Brunet JF, Goridis C, Warth R, Barhanin J (2010) Task2 potassium channels set central respiratory CO_2 and O_2 sensitivity. Proc Natl Acad Sci U S A 107:2325–2330
18. Gierten J, Hassel D, Schweizer PA, Becker R, Katus HA, Thomas D (2012) Identification and functional characterization of zebrafish K_{2P}10.1 (TREK2) two-pore-domain K^+ channels. Biochim Biophys Acta 1818:33–41
19. Hibino H, Inanobe A, Furutani K, Murakami S, Findlay I, Kurachi Y (2010) Inwardly rectifying potassium channels: their structure, function, and physiological roles. Physiol Rev 90:291–366
20. Huckstepp RT, Dale N (2011) CO_2-dependent opening of an inwardly rectifying K^+ channel. Pflugers Arch 461:337–344
21. Ishimatsu A, Iwama GK, Bentley DB, Heisler N (1992) Contribution of the secondary circulatory system to acid–base regulation during hypercapnia in rainbow trout (*Onchrryncus mykiss*). J Exp Biol 170:43–56
22. Ito Y, Kobayashi S, Nakamura N, Miyagi H, Esaki M, Hoshijima K, Hirose S (2013) Close association of carbonic anhydrase (CA2a and CA15a), Na^+/H^+ exchanger (Nhe3b), and ammonia transporter Rhcg1 in zebrafish ionocytes responsible for Na^+ uptake. Front Physiol 4:59
23. Jiang C, Rojas A, Wang R, Wang X (2005) CO_2 central chemosensitivity: why are there so many sensing molecules? Respir Physiol Neurobiol 145:115–126
24. Jonz MG, Fearon IM, Nurse CA (2004) Neuroepithelial oxygen chemoreceptors of the zebrafish gill. J Ph 560:737–752
25. Kim Y, Bang H, Gnatenco C, Kim D (2001) Synergistic interaction and the role of C-terminus in the activation of TRAAK K^+ channels by pressure, free fatty acids and alkali. Pflugers Arch 442:64–72
26. Lesage F, Guillemare E, Fink M, Duprat F, Lazdunski M, Romey G, Barhanin J (1996) TWIK-1, a ubiquitous human weakly inward rectifying K^+ channel with a novel structure. EMBO J 15:1004–1011
27. Lesage F, Terrenoire C, Romey G, Lazdunski M (2000) Human TREK2, a 2P domain mechano-sensitive K^+ channel with multiple regulations by polyunsaturated fatty acids, lysophospholipids, and Gs, Gi, and Gq protein-coupled receptors. J Biol Chem 275:28398–28405
28. López-Barneo J, Ortega-Sáenz P, Pardal R, Pascual A, Piruat JI (2008) Carotid body oxygen sensing. Eur Respir J 32:1386–1398
29. Maingret F, Patel AJ, Lesage F, Lazdunski M, Honore E (1999) Mechano- or acid stimulation, two interactive modes of activation of the TREK-1 potassium channel. J Biol Chem 274:26691–26696
30. Mölich A, Heisler N (2005) Determination of pH by microfluorometry: intracellular and interstitial pH regulation in developing early-stage fish embryos (*Danio rerio*). J Exp Biol 208:4137–4149
31. Mulkey DK, Stornetta RL, Weston MC, Simmons JR, Parker A, Bayliss DA, Guyenet PG (2004) Respiratory control by ventral surface chemoreceptor neurons in rats. Nat Neurosci 7:1360–1369
32. Mulkey DK, Talley EM, Stornetta RL, Siegel AR, West GH, Chen X, Sen N, Mistry AM, Guyenet PG, Bayliss DA (2007) TASK channels determine pH sensitivity in select respiratory neurons but do not contribute to central respiratory chemosensitivity. J Neurosci 27: 14049–14058
33. Nattie E, Li A (2009) Central chemoreception is a complex system function that involves multiple brain stem sites. J Appl Physiol 106: 1464–1466
34. Niemeyer MI, Cid LP, Barros LF, Sepúlveda FV (2001) Modulation of the two-pore domain acid-sensitive K^+ channel TASK-2 (KCNK5) by changes in cell volume. J Biol Chem 276:43166–43174

35. Niemeyer MI, Cid LP, Peña-Münzenmayer G, Sepúlveda FV (2010) Separate gating mechanisms mediate the regulation of K_{2P} potassium channel TASK-2 by intra- and extracellular pH. J Biol Chem 285: 16467–16475
36. Niemeyer MI, González-Nilo FD, Zúñiga L, González W, Cid LP, Sepúlveda FV (2007) Neutralization of a single arginine residue gates open a two-pore domain, alkali-activated K^+ channel. Proc Natl Acad Sci U S A 104:666–671
37. Ortega-Sáenz P, Levitsky KL, Marcos-Almaraz MT, Bonilla-Henao V, Pascual A, López-Barneo J (2010) Carotid body chemosensory responses in mice deficient of TASK channels. J Gen Physiol 135: 379–392
38. Perry SF, Abdallah S (2012) Mechanisms and consequences of carbon dioxide sensing in fish. Respir Physiol Neurobiol 184: 309–315
39. Putnam RW, Filosa JA, Ritucci NA (2004) Cellular mechanisms involved in CO_2 and acid signaling in chemosensitive neurons. Am J Physiol 287:C1493–C1526
40. Qin Z, Lewis JE, Perry SF (2010) Zebrafish (*Danio rerio*) gill neuroepithelial cells are sensitive chemoreceptors for environmental CO_2. J Physiol 588:861–872
41. Reyes R, Duprat F, Lesage F, Fink M, Salinas M, Farman N, Lazdunski M (1998) Cloning and expression of a novel pH-sensitive two pore domain K^+ channel from human kidney. J Biol Chem 273: 30863–30869
42. Roos A, Boron WF (1981) Intracellular pH. Physiol Rev 61:296–434
43. Trapp S, Aller MI, Wisden W, Gourine AV (2008) A role for TASK-1 (KCNK3) channels in the chemosensory control of breathing. J Neurosci 28:8844–8850
44. Trapp S, Tucker SJ, Gourine AV (2011) Respiratory responses to hypercapnia and hypoxia in mice with genetic ablation of Kir5.1 (*Kcnj16*). Exp Physiol 96:451–459
45. Vince JW, Reithmeier RA (1998) Carbonic anhydrase II binds to the carboxyl terminus of human band 3, the erythrocyte Cl^-/HCO_3^- exchanger. J Biol Chem 273:28430–28437
46. Wang W, Pizzonia JH, Richerson GB (1998) Chemosensitivity of rat medullary raphe neurones in primary tissue culture. J Physiol 511: 433–450
47. Warth R, Barrière H, Meneton P, Bloch M, Thomas J, Tauc M, Heitzmann D, Romeo E, Verrey F, Mengual R, Guy N, Bendahhou S, Lesage F, Poujeol P, Barhanin J (2004) Proximal renal tubular acidosis in TASK2 K^+ channel-deficient mice reveals a mechanism for stabilizing bicarbonate transport. Proc Natl Acad Sci U S A 101: 8215–8220
48. Wu J, Xu H, Shen W, Jiang C (2004) Expression and coexpression of CO_2-sensitive Kir channels in brainstem neurons of rats. J Membr Biol 197:179–191
49. Xu H, Cui N, Yang Z, Qu Z, Jiang C (2000) Modulation of Kir4.1 and Kir5.1 by hypercapnia and intracellular acidosis. J Physiol 524:725–735
50. Yuan Y, Shimura M, Hughes BA (2003) Regulation of inwardly rectifying K^+ channels in retinal pigment epithelial cells by intracellular pH. J Physiol 549:429–438